

(hep-ph/0009231)

YUMS 00-09, KIAS P00060, SNUTP 00-024

Enhancement of the Higgs pair production at the LHC; the MSSM and extra dimension effects

C. S. Kim ^{a,b}, Kang Young Lee ^c and Jeonghyeon Song ^c^a*Department of Physics and IPAP, Yonsei University, Seoul 120-749, Korea*^b*Department of Physics, University of Wisconsin, Madison, WI 53706, USA*^c*School of Physics, Korea Institute for Advanced Study, Seoul 130-012, Korea*

Abstract

The neutral Higgs pair production at the LHC is studied in the MSSM, the large extra dimensional (ADD) model and the Randall-Sundrum (RS) model, where the total cross section can be significantly enhanced compared to that in the SM. The p_T , invariant mass and rapidity distributions of each model have been shown to be distinctive: The ADD model raises the p_T and invariant mass distributions at high scales of p_T and invariant mass; in the RS model resonant peaks appear after the SM contribution dies away; the SM and the MSSM distributions drop rapidly at those high scales; in the ADD and the RS models the rapidity distributions congregate more around the center. It is concluded that various distributions of the Higgs pair production at the LHC with restrictive kinematic cuts would provide one of the most robust signals for the extra dimensional effects.

PACS numbers: 04.50.+h, 12.60.-i, 13.85.-t, 13.90.+i

I. INTRODUCTION

The standard model (SM) has been very successful in explaining experimental signals, including recent results from the CERN LEP-II collider [1]. Nevertheless one of the most important ingredients of the SM, the Higgs mechanism, has not been experimentally probed yet; it is responsible for spontaneous electroweak symmetry breaking accompanying the mass generation of the W^\pm and Z^0 gauge bosons as well as the SM fermions. Recently, ALEPH group of the LEP-II has reported the observation of an excess of 3σ in the search of the SM Higgs boson, which corresponds to the Higgs mass about 114 GeV [2]. As operations of the LEP-II have been completed, the decision, whether the observations are only the results of statistical fluctuations or the first signal of the Higgs boson production, is suspended until the Fermilab Tevatron II and/or the CERN LHC experiments running [3]. Thus it is naturally anticipated that primary efforts of future collider experiments are to be directed toward the search for Higgs bosons [4].

In particular at hadron colliders, the pair production of Higgs bosons holds a distinctive position in understanding the Higgs mechanism [5]. First, it may provide the experimental reconstruction of the Higgs potential, as the triple self-coupling of Higgs particles is involved. The establishment of the Higgs' role in the electroweak symmetry breaking is crucially dependent on this measurement. Second, the signal-to-background ratio is significantly improved compared to that of a single Higgs boson production. The invariant mass scale of the *single* Higgs production is fixed by the Higgs mass, of order ~ 100 GeV. Thus their detection through heavy quark decay modes suffers from large QCD backgrounds. Besides, one viable decay mode $h \rightarrow \gamma\gamma$ has a very small branching ratio of order 10^{-3} [6]. For the *pair* production of the Higgs particles, the four b -jets in the final states are energetic, reducing the main background $h b\bar{b}$ with soft b -jets [7]. Third, this is a rare process in the sense that the effects of physics beyond the SM can remarkably enhance the cross section with respect to that in the SM; the minimal supersymmetric standard model (MSSM) [8] provides some parameter space for the large enhancement of the total cross section, which

should accommodate the large Yukawa coupling of the b quarks, the resonant decay of $H \rightarrow hh$, and/or dominantly large contribution of the squark loops [7]; extra dimensional models provide tree level diagrams mediated by the Kaluza-Klein (KK) gravitons, leading to large total cross sections. In fact, these new theoretical approaches have drawn extensive attention as candidates for the solution of the gauge hierarchy problem, the existence and stability of the enormous hierarchy between the electroweak and Planck scales. Therefore, it is worth studying the production of a neutral Higgs pair with the effects of the MSSM and the extra dimensional models, and finding the characteristic distribution of each model. We shall restrict ourselves to the procedure at the LHC, which is scheduled to start operating in 2005. Despite the assurance of the detectability of the lightest CP-even MSSM Higgs boson with $\sqrt{s} \gtrsim 250$ GeV and $\int \mathcal{L} dt \gtrsim 10 \text{ fb}^{-1}$ [9], the LHC takes a practical advantage over the future e^+e^- linear colliders which lack specific plans yet.

The remainder of the paper is organized as follows. The next section details the neutral Higgs pair production at the LHC in the SM, the MSSM, the large extra dimensional (ADD) model [10], and the Randall-Sundrum (RS) model [11]. In Sec. III, we discuss various distributions useful to discriminate effects of each model from others. The last section deals with a brief summary and conclusions.

II. THEORETICAL DISCUSSIONS AND FORMULAE

The production of a Higgs boson pair at a hadron collider proceeds through several modes; WW fusion, bremsstrahlung of Higgs bosons off heavy quarks, and gluon-gluon fusion. At the LHC, the gg fusion is expected to play a main role, since the gluon luminosity increases with beam energy. In this paper, we focus on the process $gg \rightarrow hh$, where the h is the lightest Higgs boson in each theory.

The invariant amplitude squared is generally written as, in terms of the helicity amplitude $\mathcal{M}_{\lambda_1\lambda_2}$ for the initial gluon helicities $\lambda_{1(2)}$ [7],

$$\overline{|\mathcal{M}|^2} = 2 \cdot \frac{1}{4} \cdot \frac{1}{64} \cdot \frac{1}{2} \left[|\mathcal{M}_{++}|^2 + |\mathcal{M}_{+-}|^2 + |\mathcal{M}_{-+}|^2 + |\mathcal{M}_{--}|^2 \right], \quad (1)$$

where the factor 2 refers the color factor $[\text{Tr}(T^a T^b)]^2 = 2$, the factor 1/4 the initial gluon helicity average, the factor 1/64 the gluon color average, and the final factor 1/2 the symmetry factor for the two identical Higgs boson production. For the processes with CP conservation, the helicity amplitudes are related as $\mathcal{M}_{++} = \mathcal{M}_{--}$ and $\mathcal{M}_{+-} = \mathcal{M}_{-+}$.

For the numerical analysis, we use the leading order MRST parton distribution functions (PDF) for a gluon in a proton [12]. The QCD factorization and renormalization scales Q are set to be the hh invariant mass, *i.e.*, $\sqrt{\hat{s}}$. The Q^2 -dependence is expected to be small on the distribution shapes, which are of our main interest. The center-of-momentum (c.m.) energy at pp collisions is $\sqrt{s} = 14$ TeV. And we have employed the kinematic cuts of $p_T \geq 25$ GeV and $|\eta| \leq 2.5$ throughout the paper.

A. In the SM

In the SM, there are two types of Feynman diagrams as depicted in Fig. 1. One is the triangle diagram where a virtual Higgs boson, produced from gg fusion through heavy quark triangles, decays into a pair of Higgs bosons. The other is the box diagram where the Higgs pair is produced through heavy quark boxes. It is to be noted that the triangle diagram incorporates the triple self-coupling of Higgs bosons. For analytic expressions of all the one-loop helicity amplitudes of the process $gg \rightarrow hh$, we refer the reader to Refs. [7,5]. Fig. 2 shows the total cross section of the SM Higgs pair production at the LHC, as a function of the Higgs mass m_h . At $m_h \simeq 100$ GeV, the σ_{tot} is of order 60 fb, which decreases rapidly with increasing m_h .

B. In the MSSM

The existence of a fundamental scalar particle in the SM causes the well-known gauge hierarchy problem. Traditional approaches are to introduce new symmetries, motivated by the chiral symmetry for light fermion masses and the gauge symmetries for gauge boson masses. Supersymmetry is one of the most popular candidates for this new symmetry.

The MSSM Higgs pair production undergoes distinctive contributions coming from the new Higgs and squark sectors, which provide the possibilities to greatly enhance the total cross section of the process. First, two doublets and thus two different vacuum expectation values of the Higgs fields allow the Yukawa coupling of the b quark to be compatible with that of the top quark, which corresponds to the large $\tan\beta$ case. Much smaller mass of the b quark may makes its loop contribution even larger than the top quark contribution [5]. Second, two Higgs doublets imply the presence of a heavy CP-even neutral Higgs boson H , which can decay into two light Higgs bosons if kinematically allowed. This resonant contribution $gg \rightarrow H \rightarrow hh$ is shown to enhance the total cross section with respect to the SM case by about an order of magnitude. Third, the MSSM permits a parameter space where the \tilde{b} or \tilde{t} loop contributions can exceed the SM quark loop contributions by more than two orders of magnitude [7]. For the maximization of squark loop contributions which occurs through the \tilde{b} loops, this parameter space should allow large value of $\tan\beta$, considerably light \tilde{b}_1 mass, and large mass of A and/or $|\mu|$. Since the third enhancement possibility has rather restrictive parameter space (for example, the squark loop contributions are practically negligible unless $m_{\tilde{b}_1} \lesssim 120$ GeV), we consider only the quark loop contributions, as in Ref. [5]. The corresponding Feynman diagrams are the same as the SM case, except for the different coupling strengths and the presence of the neutral heavy Higgs boson H (see Fig. 1).

The MSSM total cross section as a function of the Higgs mass shows similar behavior to that of the SM, except for the overall enhancement, as shown in Ref. [5]. As anticipated, the total cross sections in the large and small $\tan\beta$ cases are much increased compared to the SM case. In particular, the large $\tan\beta$ value with $m_h \simeq 100$ GeV leads to an order of magnitude enhancement of the cross section.

C. In the ADD model

The gauge hierarchy problem has been approached without resort to any new symmetry by Arkani-Hamed, Dimopoulos, and Dvali (ADD) [10]. One prerequisite of the hierarchy problem itself is removed; the Planck mass is not fundamental; the nature allows only one fundamental mass scale M_S which is at the electroweak scale. By introducing the $N \geq 2$ extra dimensional compact space, the observed huge Planck mass is attributed to the large volume of the extra space, since $M_{\text{Pl}}^2 \simeq M_S^{N+2} R^N$ where the R is the size of the extra dimension. The prohibition of the SM particles' escaping into the extra space can be achieved by describing the matter fields as open strings of which the end-points are fixed to our four-dimensional world.

Of great interest and significance is that this idea is testable at colliders. The KK reduction from the whole $(4+N)$ -dimensions to our four-dimensional world yields towers of massive KK-states in the four-dimensional effective theory. Even though the coupling of a KK-graviton to the ordinary matter fields is extremely suppressed by the Planck scale, tiny mass-splitting $\Delta m_{\text{KK}} \sim 1/R$ (which is about 10^{-3} eV for the $N = 2$ case) induces summation over all KK-states, which compensates for the Planck scale suppression. In addition to single graviton emission processes as missing energy events [13], the indirect effects of the massive graviton exchange on various collider experiments [14], and the possible Lorentz and CPT invariance violations through the change of the metric on the brane [15] have been extensively studied.

For the Higgs pair production through the gluon-gluon fusion, there exists a tree level Feynman diagram mediated by spin-2 KK-gravitons (see Fig. 3). Based on the effective four-dimensional Lagrangian [16,17], the helicity amplitudes are obtained as

$$\mathcal{M}_{++} = \mathcal{M}_{--} = 0 , \quad (2)$$

$$\mathcal{M}_{+-} = \mathcal{M}_{-+} = \frac{16\lambda}{M_S^4} (m_h^4 - \hat{u}\hat{t}) ,$$

which are to be added to those in the SM. The interference effects between the ADD and

the SM are proportional to $1/M_S^4$, which are, at the energy scale below M_S , dominant over pure ADD effects.

There might be a concern with our ignorance of the parton mode $q\bar{q} \rightarrow hh$ mediated by the KK-gravitons. The concern appears reasonable: The characteristic parton energy scale $\sqrt{\hat{s}}$ of the process in extra dimensional models is of the order $M_S \sim \text{TeV}$, unlike a few hundred GeV scale in the SM and the MSSM; the dominant momentum fraction x may not be so small as in the SM and the MSSM cases and the magnitude of the parton distribution functions of, in particular, the valence quarks becomes substantial. In the following, we have taken into account of the parton mode $q\bar{q} \rightarrow hh$, which has the scattering amplitude squared as

$$\overline{|\mathcal{M}|^2}(q\bar{q} \rightarrow hh) = \frac{1}{9M_S^8}(\hat{t} - \hat{u})^2(\hat{t}\hat{u} - m_h^4). \quad (3)$$

According to our numerical analysis, the contribution of $q\bar{q} \rightarrow hh$ mode turns out to be at most a few percent to the total cross sections, because the amplitude squared itself is smaller than that of $gg \rightarrow hh$ mode (by a factor of about $1/36$) while, at TeV $\sqrt{\hat{s}}$, the PDF of a valence quark and a sea quark is of the same order with that of two gluons.

Note that in the parton c.m. frame, the nonzero helicity amplitude can be written as

$$\mathcal{M}_{+-}|_{\text{gg-c.m.}} = -\frac{16\lambda}{M_S^4} p_T^2 \hat{s}, \quad (4)$$

where the p_T is the transverse momentum of an outgoing Higgs particle. Unitarity is apparently violated at high energies, which is expected from the use of an effective Lagrangian. It is reasonable that we only consider the region where our perturbative calculations are reliable, which can be achieved by excluding the region with high invariant mass. In Ref. [18], the partial wave amplitudes of the elastic process $\gamma\gamma \rightarrow \gamma\gamma$ in the ADD model have been examined, yielding the bound on the ratio $M_S/\sqrt{\hat{s}}$, and a valid region is conservatively found to be $\sqrt{\hat{s}} \leq 0.9M_S$. In the following analyses, we impose an additional kinematic bound such as

$$M_{hh} < 0.9 M_S.$$

In Fig. 2, we present the total cross section as a function of m_h with $M_S = 2.5$ TeV. As expected from the presence of a tree level diagram in the ADD model, the total cross section is substantially increased with respect to the SM case. For a pair production of Higgs bosons with mass 115 GeV, we have obtained

$$\frac{\sigma_{\text{SM+ADD}}(m_h = 115 \text{ GeV}, M_S = 2.5 \text{ TeV})}{\sigma_{\text{SM}}(m_h = 115 \text{ GeV})} \approx 1.72. \quad (5)$$

We note that the ADD effects lead to a gentle drop-off of the σ_{tot} with respect to the Higgs boson mass, contrary to the rapid decrease in the SM. Thus, if the Higgs mass is large, the ADD model could still produce substantially large number of Higgs pairs at the LHC unlike in the SM case.

D. In the RS model

More recently, Randall and Sundrum (RS) have proposed another extra dimensional scenario where, without the *large* volume of the extra dimensions, the hierarchy problem is solved by a geometrical exponential factor, called a warp factor [11]. The spacetime in this model has a single S^1/Z_2 orbifold extra dimension with the metric

$$ds^2 = e^{-2kr_c|\phi|} \eta_{\mu\nu} dx^\mu dx^\nu + r_c^2 d\phi^2, \quad (6)$$

where the ϕ is confined to $0 \leq |\phi| \leq \pi$. The r_c is the compactification radius which is to be stabilized by an appropriate mechanism [19]. Two orbifold fixed points accommodate two three-branes, the hidden brane at $\phi = 0$ and our visible brane at $|\phi| = \pi$ or *vice versa*. The allocation of our brane at $|\phi| = \pi$ renders a fundamental scale m_0 to appear as the four-dimensional physical mass $m = e^{-kr_c\pi} m_0$, which answers the hierarchy problem. And the effective Planck mass is

$$M_{\text{Pl}}^2 = (M^3/k)(1 - e^{-2kr_c\pi}),$$

where the M is the five-dimensional Planck scale. Note that all of the M_{Pl} , k , and M are of the Planck scale.

The compactification of the fifth dimension leads to the following interaction Lagrangian in the four-dimensional effective theory [20],

$$\mathcal{L} = -\frac{1}{M_{\text{Pl}}} T^{\mu\nu}(x) h_{\mu\nu}^{(0)}(x) - \frac{1}{\Lambda_\pi} T^{\mu\nu}(x) \sum_{n=1}^{\infty} h_{\mu\nu}^{(n)}(x), \quad (7)$$

where $\Lambda_\pi \equiv e^{-kr_c\pi} M_{\text{Pl}}$. Unlike almost continuous KK-graviton spectrum in the ADD model, we have one zero mode of the KK-gravitons with the coupling suppressed by the Planck scale, and the massive KK-graviton modes with the electroweak scale coupling Λ_π . The masses of the KK-gravitons are also at electroweak scale, given by [21],

$$m_n = kx_n e^{-kr_c\pi} = \frac{k}{M_{\text{Pl}}} \Lambda_\pi x_n, \quad (8)$$

where the x_n 's are the n -th roots of the Bessel function of order one.

The scattering amplitudes of the KK-mediated diagrams in the narrow width approximation can be derived from the ADD ones with the following replacement in Eq. (2) [20]:

$$\frac{\lambda}{M_S^4} \longrightarrow -\frac{1}{8\Lambda_\pi^2} \sum_{n=1}^{\infty} \frac{1}{\hat{s} - m_n^2 + im_n \Gamma_n}, \quad (9)$$

where the total decay width of the n -th KK-graviton is $\Gamma_n = \rho m_n x_n^2 (k/M_{\text{Pl}})^2$, and the ρ , fixed to be one, is a model-dependent parameter [20].

The observables based on the four-dimensional effective theory are determined by two parameters, $(\Lambda_\pi, k/M_{\text{Pl}})$. The value of k/M_{Pl} may be theoretically constrained to be less than about 0.1 [22]: The magnitude of the five-dimensional curvature, $R_5 = -20k^2$, is required to be smaller than M^2 ($\simeq M_{\text{Pl}}^2$), so that the classical RS solution derived from the leading order term in the curvature remains reliable. The Λ_π is expected to be below 10 TeV in order to explain the hierarchy problem. Unlike the M_S in the ADD case, the Λ_π does not play the role of a cut-off, relieving the concern of the unitarity violation. According to the phenomenological studies of the cross section of $e^+e^- \rightarrow \mu^+\mu^-$ in the RS model, only the case with large value of k/M_{Pl} hints the unitarity violation; even for $k/M_{\text{Pl}} \sim 1$, unitarity violation can occur at c.m. energy of several TeV [20]; the current LEP-II experiments and the Tevatron run-I have provided a lower bound of Λ_π to be about 1.5 TeV in the case of $k/M_{\text{Pl}} = 0.1$.

In Fig. 2, we plot the total cross sections with respect to the Higgs mass within the RS model. We set $\Lambda_\pi = 3$ TeV and $k/M_{\text{Pl}} = 0.1$. For the equity in comparing with the ADD case, we have employed the upper bound of $M_{hh} < 0.9 \Lambda_\pi$. Though smaller than in the ADD case, the total cross section in the RS case is larger than that in the SM:

$$\frac{\sigma_{\text{SM+RS}}(m_h = 115 \text{ GeV}, M_S = 3 \text{ TeV})}{\sigma_{\text{SM}}(m_h = 115 \text{ GeV})} \approx 1.51. \quad (10)$$

The rate of the drop-off of σ_{tot} against m_h is similar to the SM case.

In order to demonstrate the dependence of k/M_{Pl} and Λ_π , Fig. 4 shows the total cross section within the RS model as a function of Λ_π , considering three values of the ratio $k/M_{\text{Pl}} = 0.01, 0.1$ and 0.3 . The Higgs mass is set to be 100 GeV and the upper bound in M_{hh} is not applied. As the Λ_π increases, the σ_{tot} drops rapidly. And it can be seen that smaller value of the ratio k/M_{Pl} produces larger cross section. This is due to that the amplitude squared in the narrow width approximation is inversely proportional to $(k/M_{\text{Pl}})^4$ at each resonance, which yields dominant contribution.

III. NUMERICAL DISCUSSIONS AND DISTRIBUTIONS

In the previous section, we have shown the possibilities that the Higgs pair production can be greatly enhanced at the LHC. In such a circumstance, it is worthwhile to search for appropriate distributions which enable us to distinguish the contributions of one model from others. In the numerical analysis of the distributions, we have employed the following parameters: The Higgs mass is set to be 100 GeV; in the MSSM, $\tan\beta = 30$, $\mu = -640$ GeV, $M_{\tilde{t}} = M_{\tilde{b}} = 1000$ GeV, and $A_t = A_b = -410$ GeV; the M_S in the ADD model is 2.5 TeV; in the RS model, $\Lambda_\pi = 3$ TeV and $k/M_{\text{Pl}} = 0.1$.

In Fig. 5, we present the p_T -distributions in the SM and the ADD cases. While the SM p_T -distribution peaks around 150 GeV and drops rapidly with increasing p_T , the ADD effects slowly draw the distribution up at high p_T region. Note that the absence of the differential cross section at $p_T \gtrsim 1$ TeV is due the employment of the upper bound in the

M_{hh} . Fig. 6 shows the p_T -distributions in the SM and the RS cases. The presence of the Kaluza-Klein gravitons in the RS model leaves a clear shape of resonance. We caution readers that the p_T -axis is plotted by log-scale: Even if the $d\sigma^{\text{SM+RS}}/dp_T$ at $p_T > 300$ GeV, which practically vanishes in the SM, is smaller than that at $p_T < 300$ GeV by an order of magnitude, the extensive contribution at high p_T region renders the total cross section substantially enhanced. In Fig. 7, we demonstrate the MSSM p_T -distribution for the large $\tan\beta$ case. It drops rapidly with increasing p_T as in the SM case, while it peaks around 25 GeV, lower than the SM case. The magnitude of the differential cross section is shown about twenty times larger than that in the SM case.

Fig. 8 illustrates the invariant mass distributions of the Higgs pair in the SM and the ADD cases. The SM case, where the top quark loop contributions are dominant, peaks around the threshold $\sqrt{\hat{s}} \simeq 2m_t$. The ADD effects gently raise the M_{hh} -distribution at high M_{hh} region. It is expected that the blind application of the effective Lagrangian in Eq. (4) without any upper bound in M_{hh} would yield continual increase in the M_{hh} -distributions, which would show an apparent violation of unitarity. We display the M_{hh} -distribution of the RS case in Fig. 9. The high resonance peak in addition to the SM distribution implies the first KK-state of gravitons with $m_1 \simeq 750$ GeV. While at the $e^+e^- \rightarrow \mu^+\mu^-$ process the KK-gravitons appear as almost regularly spaced peaks [20], the hadronic convolution of the parton level processes obscures successive and separated peaks as the classical KK-signature. Fig. 10 displays the M_{hh} -distribution of the MSSM case with large $\tan\beta$, which undergoes dominant contributions from b quarks. Thus a peak appears just above the kinematic threshold, $\sqrt{\hat{s}} \simeq 2m_h$.

Finally, we illustrate the rapidity distributions in Fig. 11. It can be seen that the extra dimensional models produce a Higgs pair somewhat more centrally in rapidity than the SM and the MSSM do. More restrictive cut on η , such as $\eta \leq 1.0$, would eliminate a substantial portion of the SM and the MSSM contributions.

IV. CONCLUSIONS

The pair production of neutral Higgs bosons from the gluon-gluon fusion at the LHC has been studied in the SM, the MSSM, the large extra dimensional model and the Randall-Sundrum model. We have shown that both the supersymmetric and extra-dimensional models can substantially enhance the total cross section of the Higgs pair production. In the MSSM case, the large $\tan \beta$ value makes possible the b -quark contribution dominant over the top quark contribution and the resonant decay of a heavy Higgs particle into two light Higgs particle. The extra dimensional models allow tree level Feynman diagrams mediated by the Kaluza-Klein gravitons, which significantly increase the total cross section. Since the ADD model has been shown to undergo the violation of partial wave unitarity at high energies, we have employed an upper bound in the invariant mass of two Higgs bosons, which is obtained from the analysis of the J -partial wave amplitudes of the elastic process $\gamma\gamma \rightarrow \gamma\gamma$. In addition, it was shown that the total cross section in the ADD case with the upper bound in M_{hh} decreases gently with increasing Higgs mass, whereas those in the SM, the MSSM and the RS cases decrease rapidly.

If Higgs pairs are produced at hadron colliders much more than the SM prediction, the three non-standard models considered here are good candidates for the explanation. We have demonstrated the p_T , invariant mass and rapidity distributions of each case. The distribution shapes are shown to be different for each model, providing valuable criteria to distinguish the contribution of one model from others. The p_T -distribution in the SM peaks and drops rapidly; the MSSM one for the large $\tan \beta$ case peaks just above the threshold of p_T and also drops rapidly; the ADD effects induce a slow raising after the SM peak; the RS effects can be discovered by the presence of a resonance peak. The invariant mass distributions are similar to the p_T -distributions: The SM and the MSSM have peaks around a few hundred GeV; the ADD effects gently raise the M_{hh} -distribution at high energies; the RS contribution yields a series of resonant peaks. Therefore, restrictive cuts on the p_T and M_{hh} would eliminate the main contributions of the SM and the MSSM cases, which provides

one of the most straightforward methods to signal the existence of low scale quantum gravity effects. Finally, the rapidity distributions in the ADD and the RS models show significantly narrow peaks around $\eta = 0$, which implies the large contributions at high p_T region.

ACKNOWLEDGMENTS

We thank G. Cvetic and P. Zerwas for careful reading of the manuscript and valuable comments. The work of C.S.K. was supported in part by BK21 Program, SRC Program and Grant No. 2000-1-11100-003-1 of the KOSEF, and in part by the KRF Grants, Project No. 2000-015-DP0077. The research of J.S. was supported by the BK21 Program for the Seoul National University.

REFERENCES

- [1] For a recent review, see, e.g., J. Ellis, hep-ph/0007161.
- [2] R. Barate et al., ALEPH collaboration, Phys. Lett. B **295**, 1 (2000.)
- [3] J. Ellis, hep-ex/0011086.
- [4] See, e.g., J. F. Gunion, H. E. Haber, G. L. Kane and S. Dawson, *The Higgs Hunter's Guide* (Addison-Wesley, Reading, MA, 1990).
- [5] T. Plehn, M. Spira, and P.M. Zerwas, Nucl. Phys. **B479**, 46 (1996); Erratum, *ibid.* **B531**, 655 (1998).
- [6] J. F. Gunion, G. Gamberini and S. F. Novaes, Phys. Rev. D **38**, 3481 (1988).
- [7] A. Belyaev, M. Drees, O. J .P. Éboli, J. K. Mizukoshi and S. F. Novaes, Phys. Rev. D **60**, 075008 (1999.)
- [8] For a review, see H. E. Haber and G. L. Kane, Phys. Rep. **117**, 75 (1985).
- [9] V. Barger, K. Cheung, R. J. N. Phillips, A. L. Stange, Phys. Rev. D **47**, 3041 (1993); A. Djouadi, W. Kilian, M. Mühlleitner and P. M. Zerwas, Eur. Phys. J. C **10**, 27 (1999;); D. J. Miller and S. Moretti, hep-ph/0001194.
- [10] N. Arkani-Hamed, S. Dimopoulos, and G. Dvali, Phys. Lett. B **429**, 263 (1998); Phys. Rev. D **59**, 086004 (1999); I. Antoniadis, N. Arkani-Hamed, S. Dimopoulos, and G. Dvali, Phys. Lett. B **436**, 257 (1998).
- [11] L. Randall and R. Sundrum, Phys. Rev. Lett. **83**, 3370 (1999); *ibid.*, 4690, (1999).
- [12] A. D. Martin, R. G. Roberts, W. J. Stirling and R. S. Thorne, Eur. Phys. J. C **14**, 133 (2000.)
- [13] E. A. Mirabelli, M. Perelstein and M. E. Peskin, Phys. Rev. Lett. **82**, 2236 (1999.)
- [14] J. L. Hewett, Phys. Rev. Lett. **82**, 4765 (1999); C. Balazs, H.-J. He, W. W. Repko and

C.-P. Yuan, Phys. Rev. Lett. **83**, 2112 (1999); K. Cheung and W.-Y. Keung, Phys. Rev. D **60**, 112003 (1999); K. Agashe and N. G. Deshpande, Phys. Lett. B **456**, 60 (1999); T. G. Rizzo and J. D. Wells, Phys. Rev. D **61**, 016007 (2000); T. G. Rizzo, Phys. Rev. D **60**, 075001 (1999); K. Y. Lee, H. S. Song and J. Song, Phys. Lett. B **464**, 82 (1999); K. Y. Lee, H. S. Song, J. Song and C. Yu, Phys. Rev. D **60**, 093002 (1999); K. Y. Lee, S. C. Park, H. S. Song, J. Song and C. Yu, Phys. Rev. D **61**, 074005 (2000).

[15] G. Dvali and M. Shifman, Phys. Rep. **320**, 107 (1999); G. Cvetic, S. K. Kang, C. S. Kim and K. Lee, Phys. Rev. D **62**, 057901 (2000.)

[16] T. Han, J. D. Lykken and R. Zhang, Phys. Rev. D **59**, 105006 (1999.)

[17] G. F. Giudice, R. Rattazzi, and J. D. Wells, Nucl. Phys. **B544**, 3 (1999).

[18] O. J. Eboli, T. Han, M. B. Magro and P. G. Mercadante, Phys. Rev. D **61**, 094007 (2000.)

[19] W. D. Goldberger and M. B. Wise, Phys. Rev. Lett. **83**, 4922 (1999).

[20] H. Davoudiasl, J. L. Hewett and T. G. Rizzo, Phys. Rev. Lett. **84**, 2080 (2000).

[21] W. D. Goldberger and M. B. Wise, Phys. Rev. D **60**, 107505 (1999.)

[22] H. Davoudiasl, J. L. Hewett and T. G. Rizzo, Phys. Lett. B **473**, 43 (2000); H. Davoudiasl, J. L. Hewett and T. G. Rizzo, hep-ph/0006041.

FIGURES

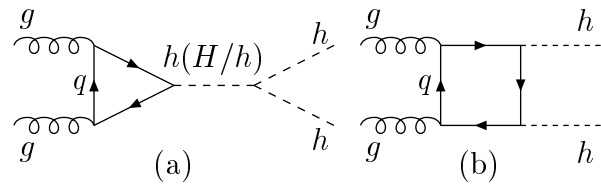


FIG. 1. The Feynman diagrams of the $gg \rightarrow hh$ process in the SM (MSSM).

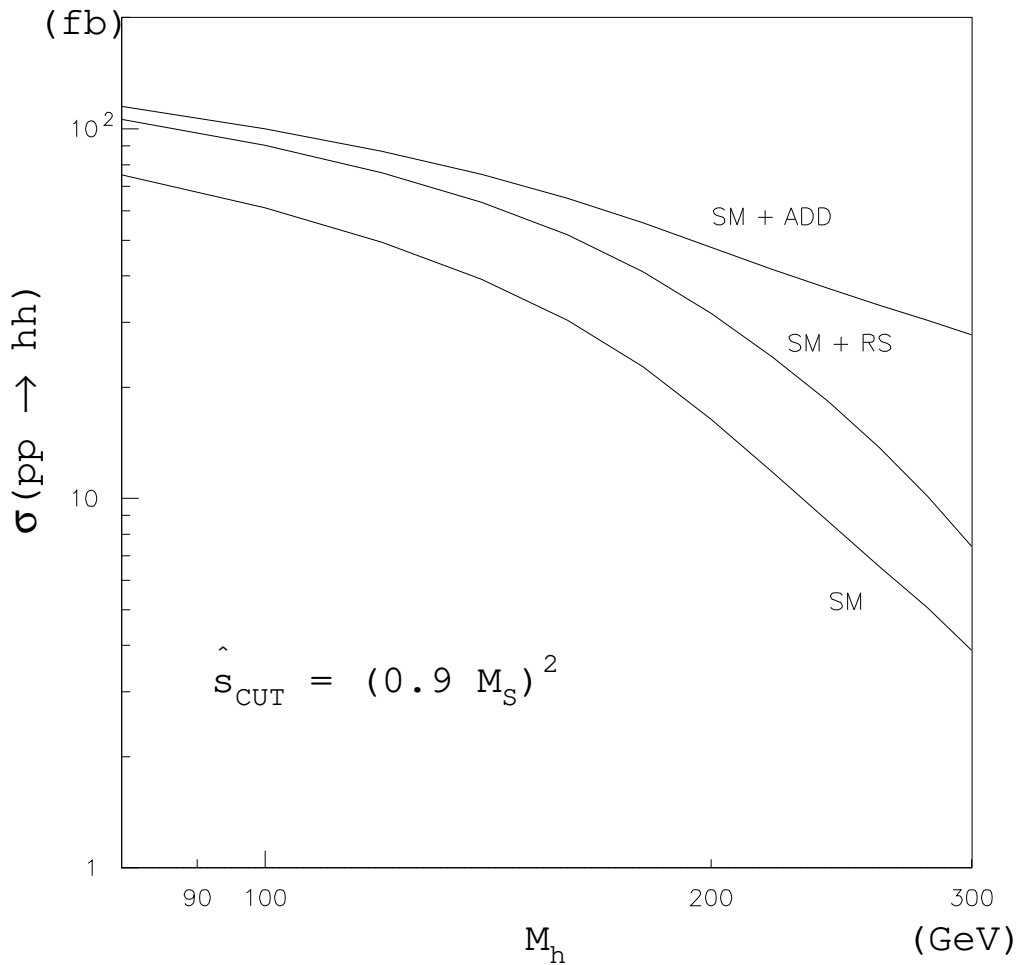


FIG. 2. The total cross section of the Higgs pair production as a function of the Higgs mass at the LHC with $\sqrt{s} = 14$ TeV in the SM, the ADD and the RS cases. The string scales are set to be $M_S = 2.5$ TeV and $\Lambda_\pi = 3$ TeV for the ADD and the RS cases, respectively. The upper bounds in $M_{hh} < 0.9 M_S(\Lambda_\pi)$ are employed.

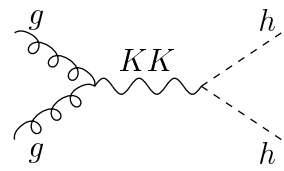


FIG. 3. The Feynman diagrams of the $gg \rightarrow hh$ in the ADD and the RS models.

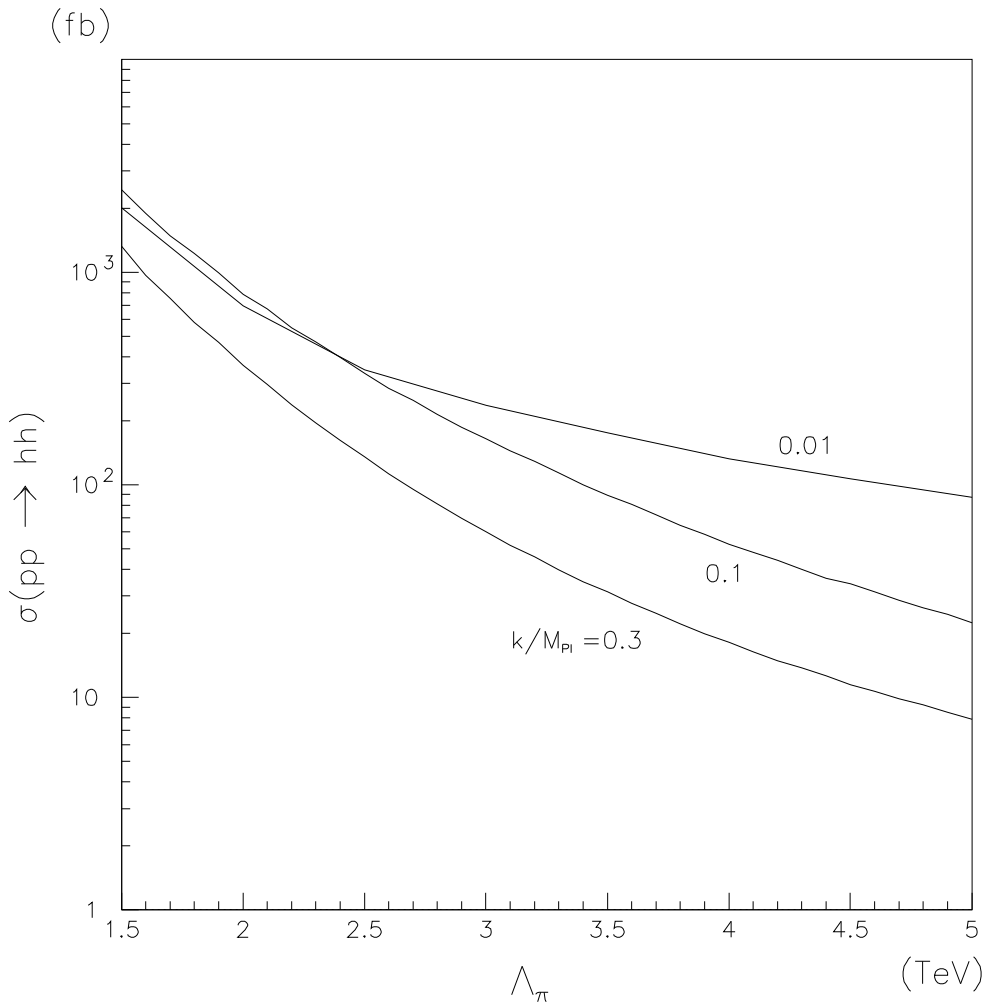


FIG. 4. The total cross sections only with the RS effects as a function of Λ_π , considering three values of the ratio $k/M_{Pl} = 0.01, 0.1$ and 0.3 .

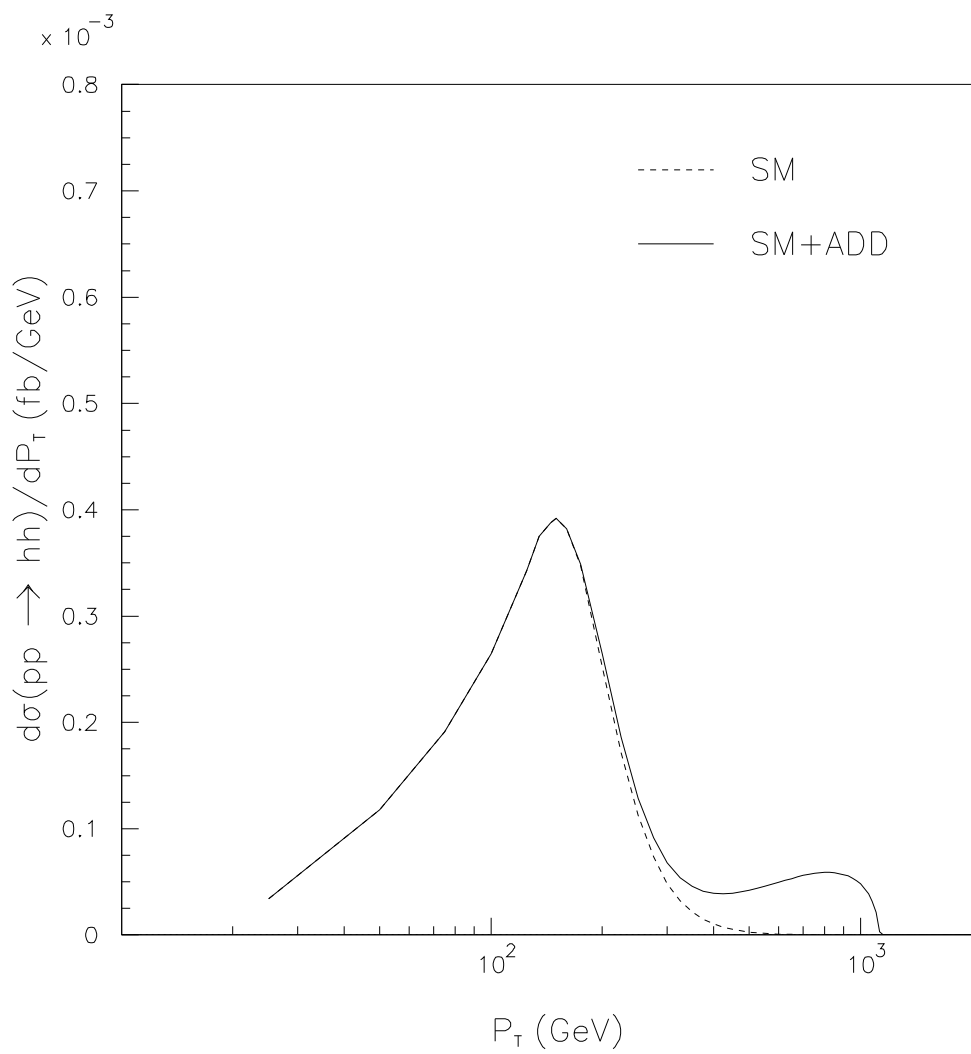


FIG. 5. The p_T distributions of the Higgs pair production in the SM, and the ADD cases.

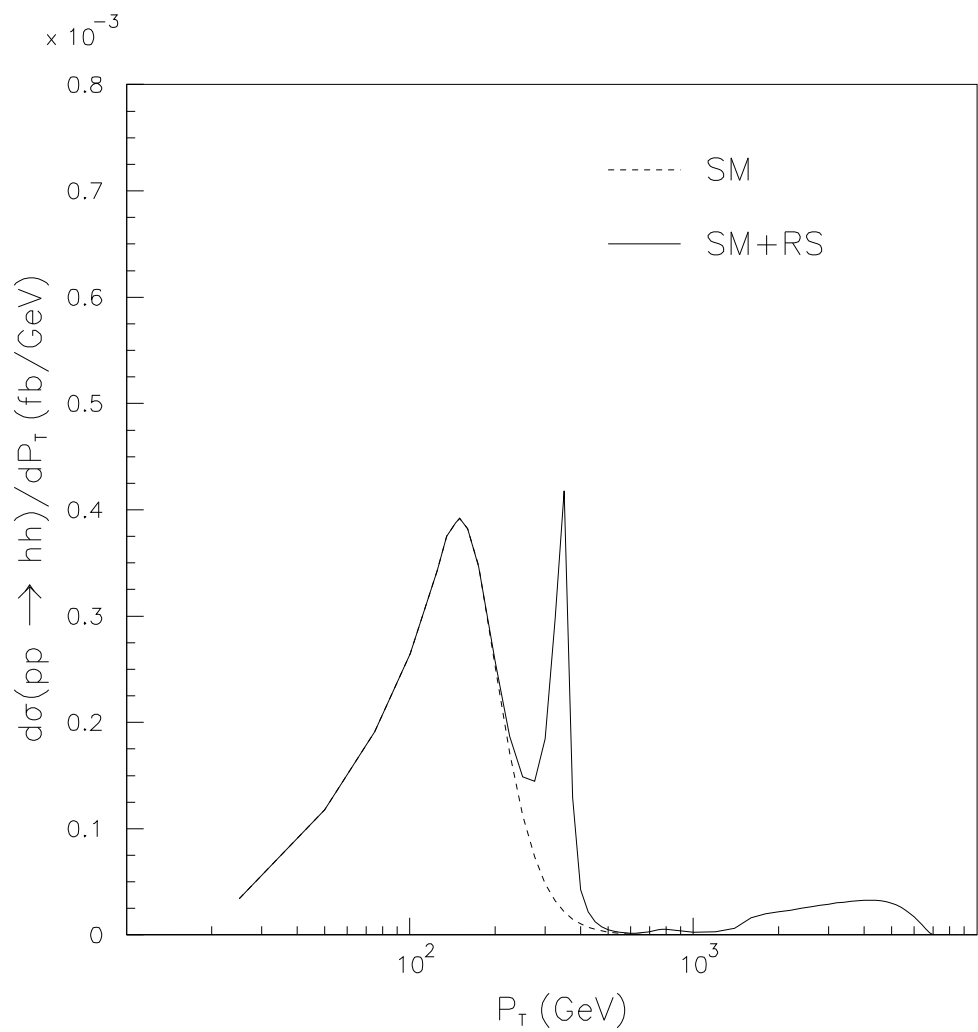


FIG. 6. The p_T distributions of the Higgs pair production in the SM and the RS cases.

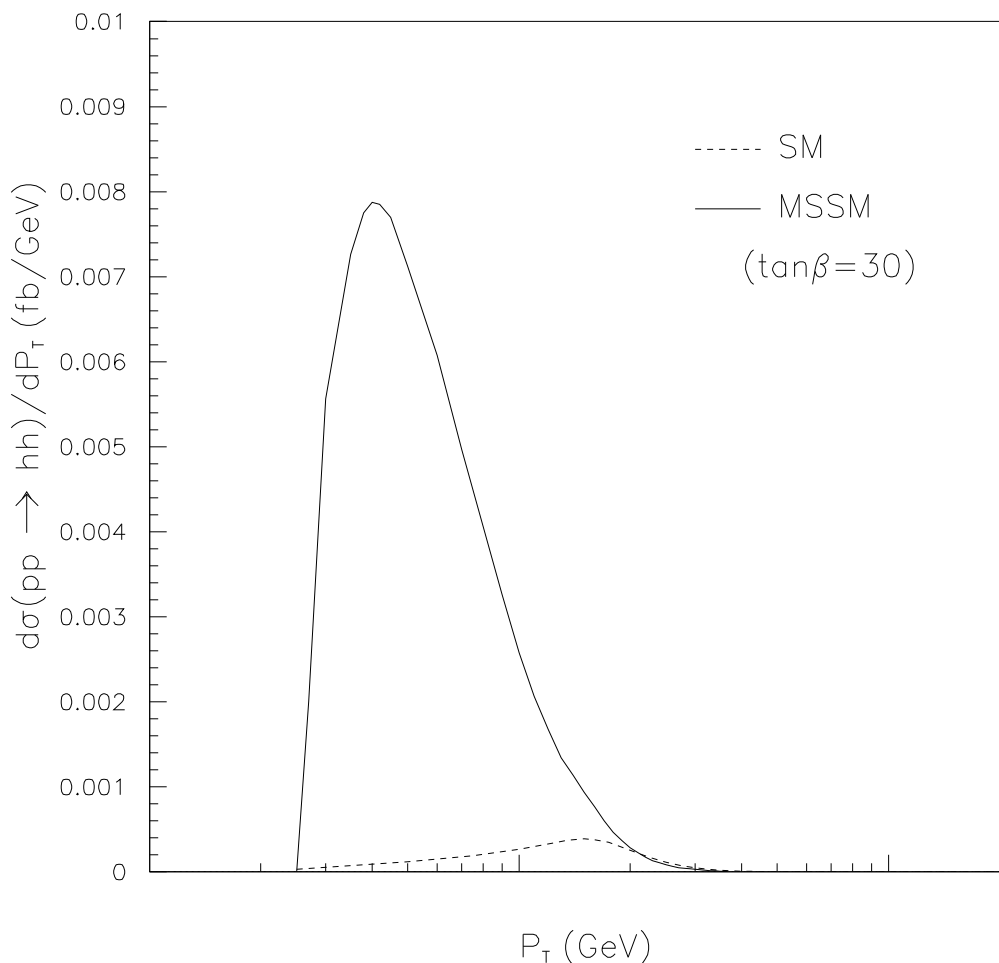


FIG. 7. The p_T distributions of the Higgs pair production in the SM, and the MSSM.

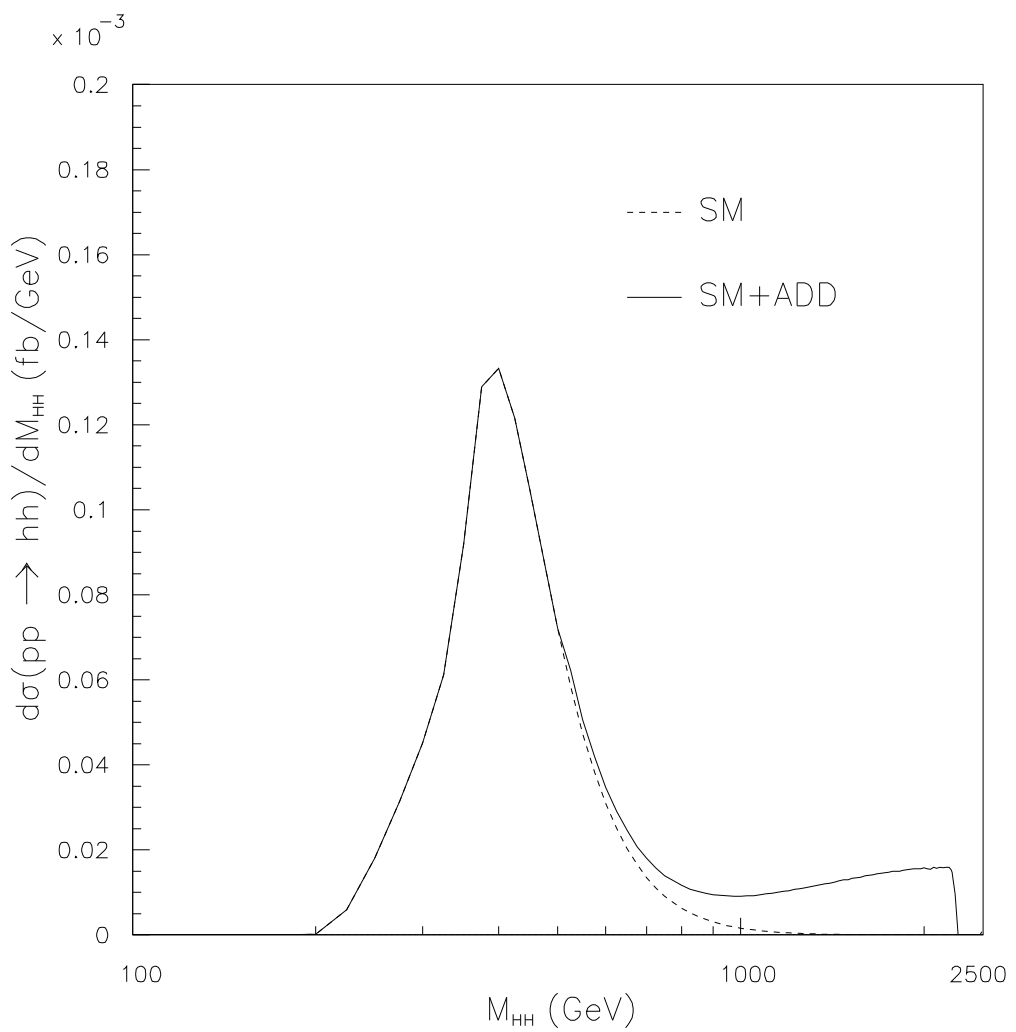


FIG. 8. The M_{hh} distributions of the Higgs pair production in the SM and the ADD cases.

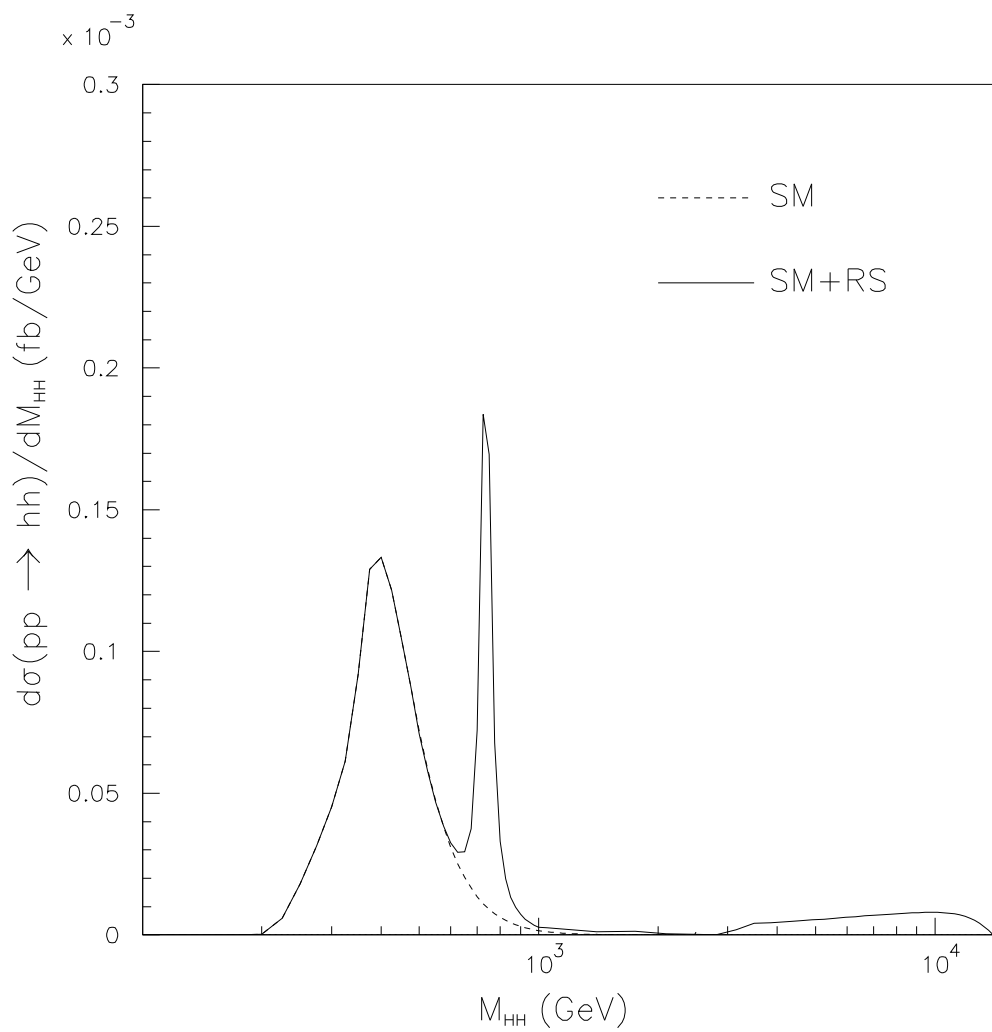


FIG. 9. The M_{hh} distributions of the Higgs pair production in the SM and the RS cases.

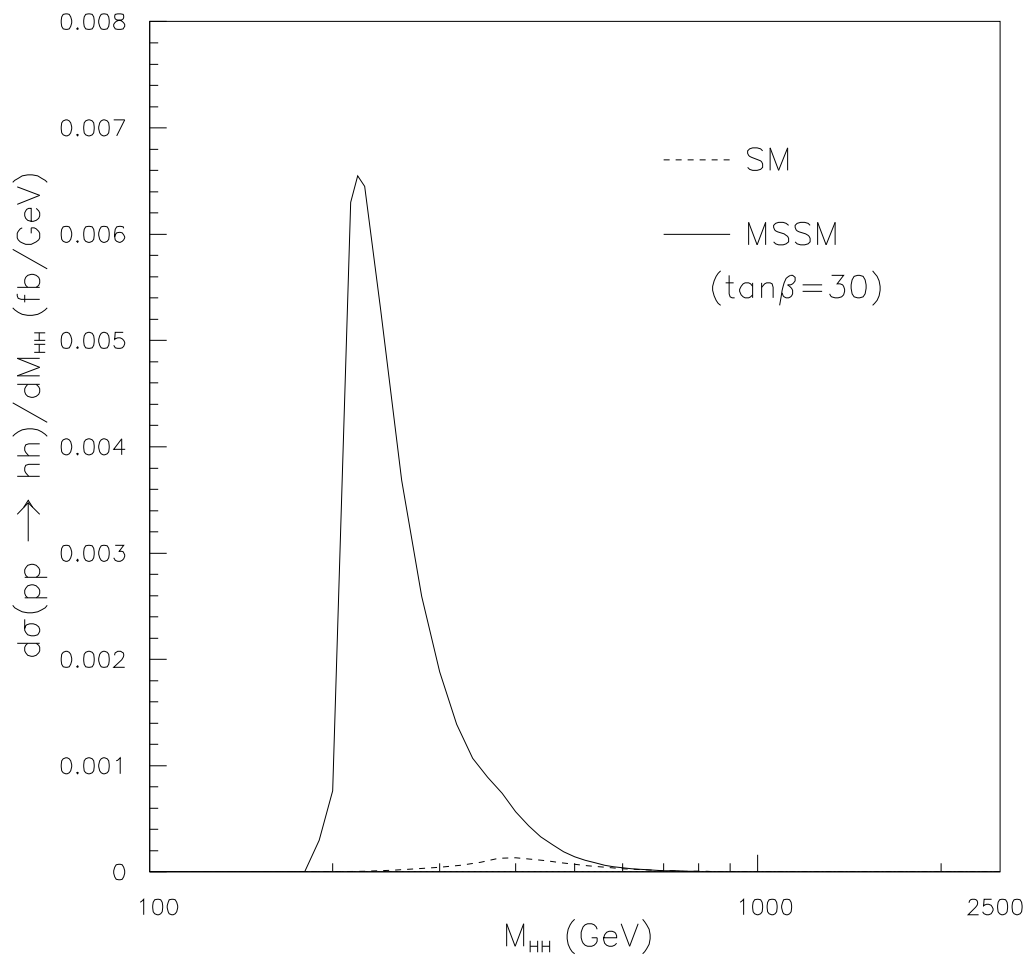


FIG. 10. The M_{hh} distributions of the Higgs pair production in the SM and the MSSM.

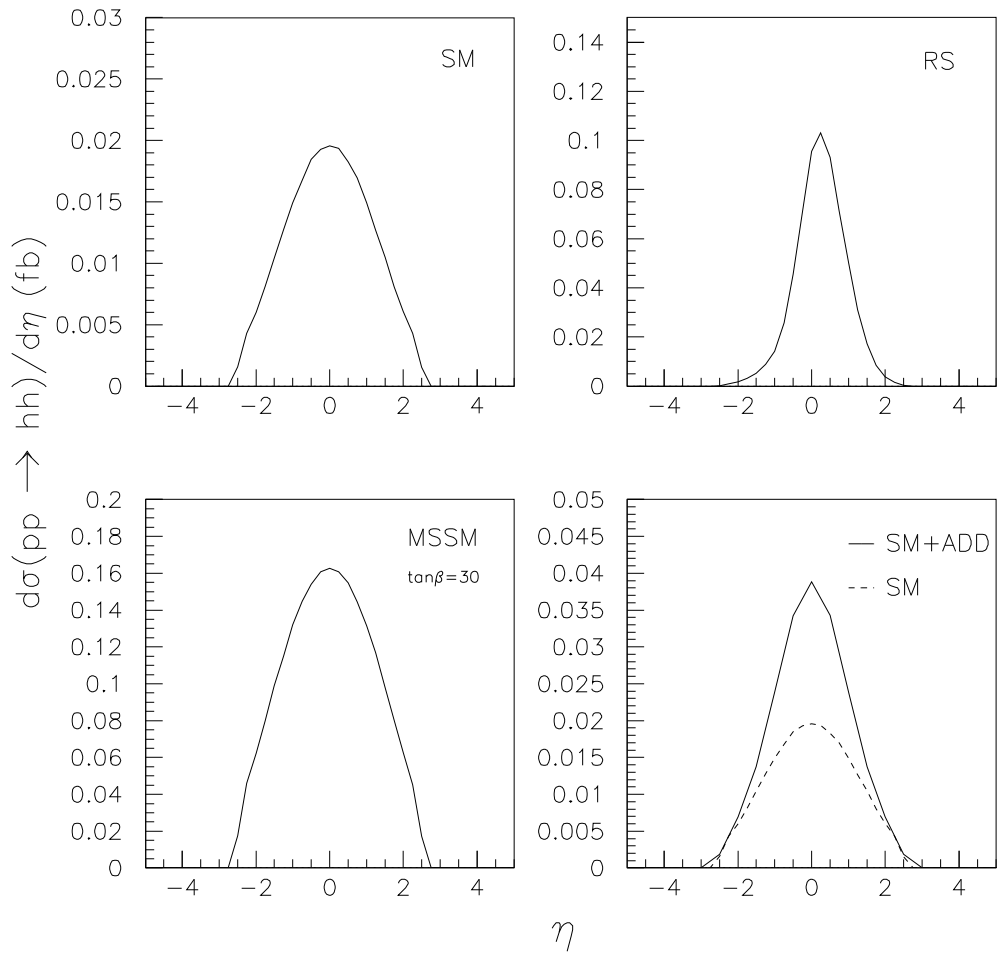


FIG. 11. The η distributions in the SM, the MSSM, the RS and the ADD cases.